Machining Science and Technology, 10:301–321

ISSN: 1091-0344 print/1532-2483 online
DOI: 10.1080/10910340600902124

Taylor & Francis
Taylor & Francis Group

ROTARY ULTRASONIC MACHINING OF TITANIUM ALLOY: EFFECTS OF MACHINING VARIABLES

N. J. Churi and Z. J. Pei □ *Department of Industrial and Manufacturing Systems Engineering, Kansas State University, Manhattan, Kansas, USA*

C. Treadwell □ *Sonic-Mill, Albuqerque, New Mexico, USA*

□ *Titanium and its alloys are finding prime applications in industries due to their unique properties. However, the high cost of machining is one of the limiting factors for their widespread use. Tremendous efforts are being made to improve the existing machining processes, and new processes are being developed to reduce the machining cost in order to increase the titanium market. However, there is no report on the systematic study of the effects of machining variables on output parameters in rotary ultrasonic machining of titanium and its alloys. This paper presents an experimental study on rotary ultrasonic machining of a titanium alloy. The cutting force, material removal rate, and surface roughness (when using rotary ultrasonic machining) of a titanium alloy have been investigated using different machining variables.*

Keywords Cutting force, Drilling, Grinding, Material Removal Rate, Rotary Ultrasonic Machining, Surface Roughness, Titanium Alloy

INTRODUCTION

Titanium is the fourth most abundant metal found in the earth's crust, and the ninth most used metal in industry (1). Titanium and its alloys are finding prime applications in defense, aerospace, and other industries due to their superior properties (such as high strength, creep strength, stability, fatigue strength, fracture toughness, fabricability, and corrosion resistance at elevated temperatures) (2).

In 1990, the total market of titanium alloy in the USA and Europe, who consume about 66% of the world's titanium (3), was 25,000 tons and 9,500 tons respectively. Figure 1 shows the proportion of titanium used in 1990 for jet engines, airframes, and industrial purposes in the USA and Europe respectively. Figure 2 shows that there was a gradual increase in the

Address correspondence to Z. J. Pei, Department of Industrial and Manufacturing Systems Engineering, Kansas State University, Manhattan, KS 66506, USA. E-mail: zpei@ksu.edu

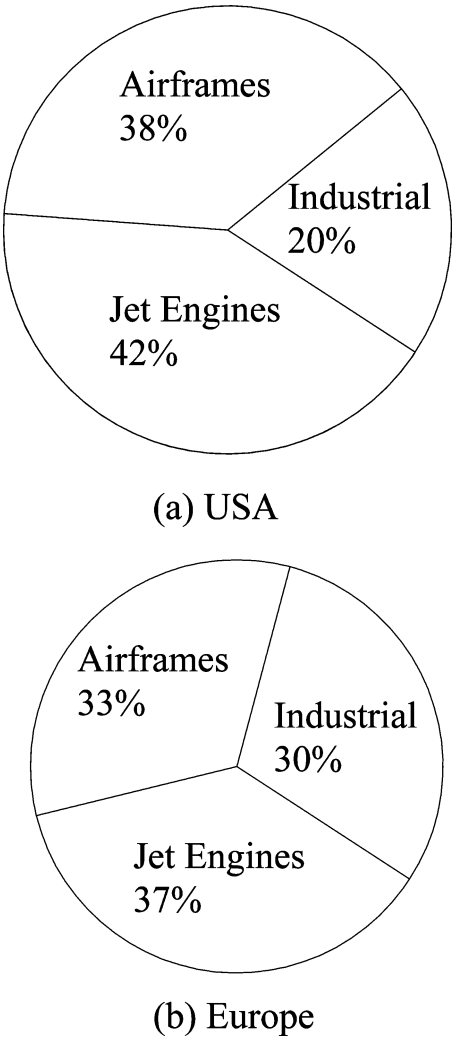

FIGURE 1 Proportion of titanium consumed in 1990 (after (1)).

titanium mill product shipment in the USA for four different market segments from 1990 to 2000 (1). In 2003, 98,000 tons of titanium and its alloys were produced worldwide (4). The major usage of titanium and its alloys is for manufacturing compressor blades, stator blades, rotors, and other parts in turbine engines (4–6). Other applications of titanium and its alloys include such industries as military (7, 8), automotive (9, 10), chemical (11, 12), medical (13, 14), and sporting goods (6, 15).

However, non-availability, increased cost of raw material, and high cost of machining (16) limit their use in industry. With the gradual increasing demand for titanium in various segments of market (Figure 2), there is a crucial need to

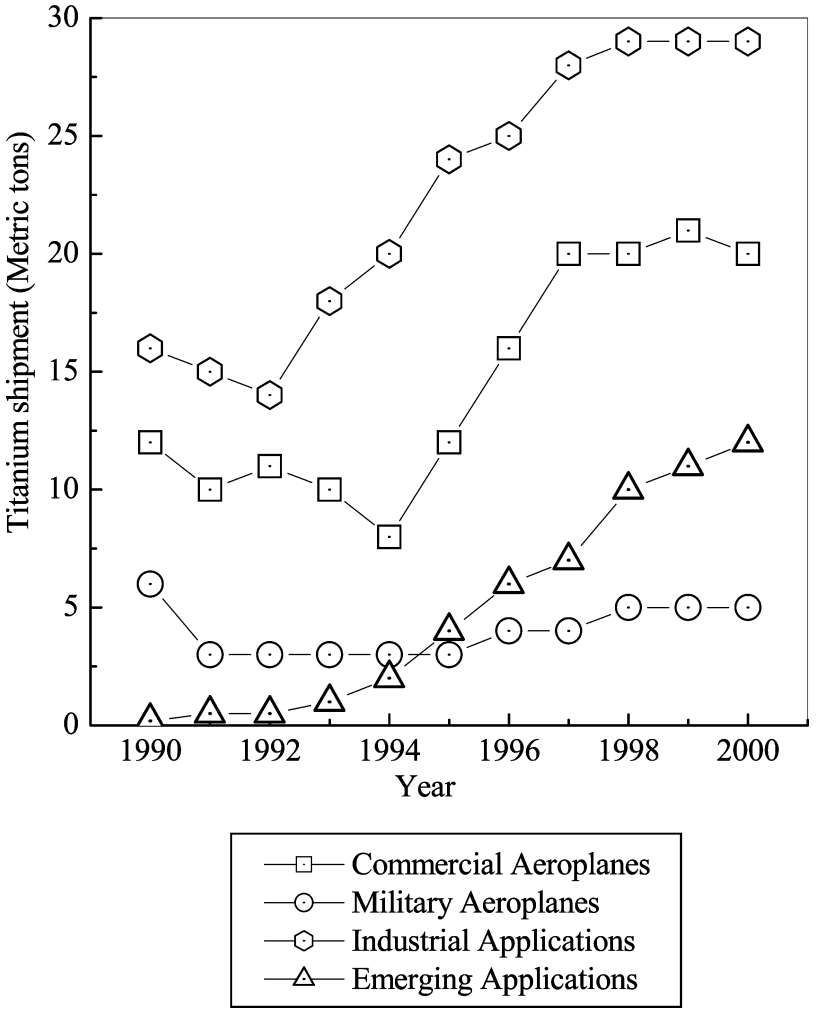

FIGURE 2 Titanium mill product shipments in the USA (after (1)).

reduce the cost of titanium products. Moreover, composite materials and amorphous alloy are being developed that may replace titanium in many applications (17–20). Under these conditions, the survival of titanium in the market and its expansion will heavily depend on reducing the cost of machining (21). Therefore, it is critically important to search new manufacturing processes that allow machining of titanium and its alloys more cost effectively.

Rotary ultrasonic machining (RUM) is one such machining process. It is a hybrid machining process that combines the material removal mechanisms of diamond grinding and ultrasonic machining. Figure 3 is the schematic illustration of rotary ultrasonic machining. A rotary core drill with metal-bonded diamond abrasives is ultrasonically vibrated and fed toward

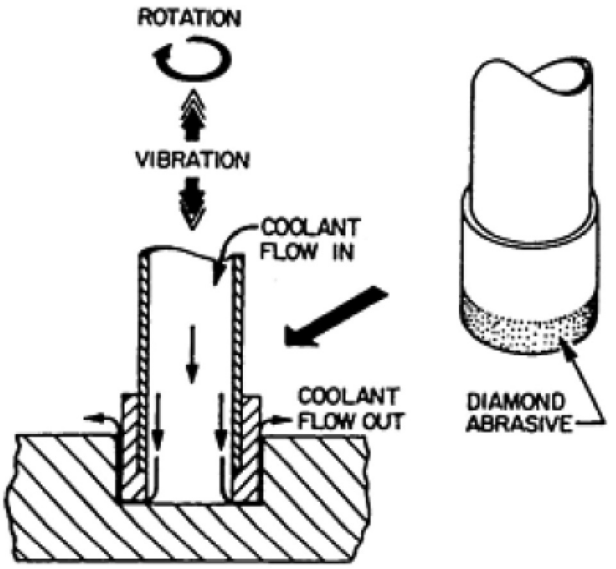

FIGURE 3 Illustration of rotary ultrasonic machining.

the workpiece at a constant feedrate or a constant force (pressure). Coolant pumped through the core of the drill washes away the swarf, prevents jamming of the drill, and keeps it cool.

Since rotary ultrasonic machining was invented in 1964 (22), the effects of its control variables (rotational speed; vibration amplitude and frequency; diamond type, size and concentration; bond type; coolant type and pressure; etc.) on its performances (material removal rate, cutting force, surface roughness, etc.) have been investigated experimentally (23–30). Efforts have also been made to develop models to predict the material removal rate in rotary ultrasonic machining from control variables (31, 32). Please note that no work has ever been reported on rotary ultrasonic machining of titanium and its alloys.

This paper reports the experimental results on the effects of spindle speed, feedrate, and ultrasonic power on cutting force, material removal rate, and surface roughness during rotary ultrasonic machining of a titanium alloy. The remainder of this paper is organized as follows. The experimental conditions and procedure are described next. Then, experimental results are presented and discussed, followed by the conclusions.

EXPERIMENTAL CONDITIONS AND PROCEDURE

Experimental Setup and Conditions

Machining experiments were performed on a machine of Sonic Mill Series 10 (Sonic-Mill, Albuquerque, NM, USA). The experimental setup

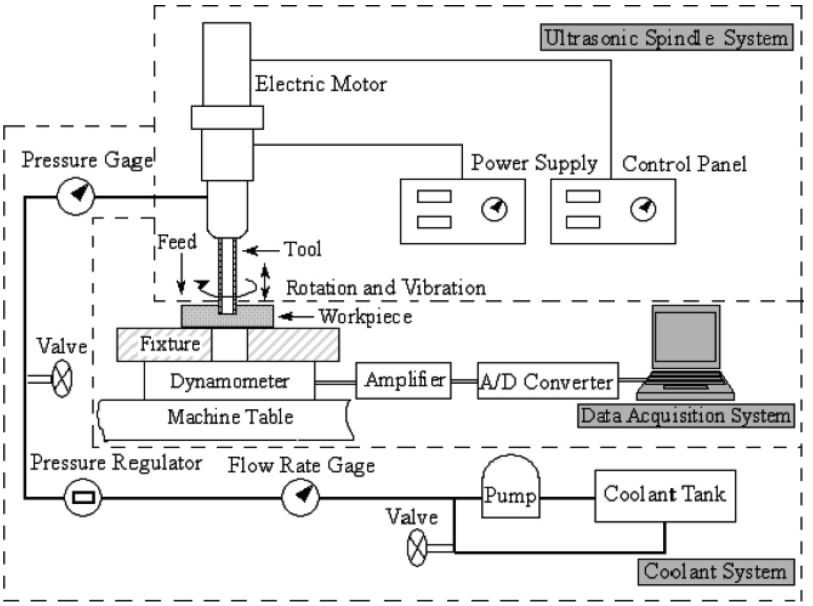

FIGURE 4 Experimental setup.

is schematically illustrated in Figure 4. It mainly consists of an ultrasonic spindle system, a data acquisition system, and a coolant system. The ultrasonic spindle system comprises of an ultrasonic spindle, a power supply, and a motor speed controller. The power supply converts 60 Hz electrical supply to high frequency (20 kHz) AC output. This is fed to the piezoelectric transducer located in the ultrasonic spindle. The ultrasonic transducer converts electrical input into mechanical vibrations. The motor attached atop the ultrasonic spindle supplies the rotational motion of the tool and different speeds can be obtained by adjusting the motor speed controller. The fixture to hold the specimens was mounted on a dynamometer that was attached to the machine table.

Table 1 shows the experimental conditions. Mobilemet S122 water-soluble cutting oil (MSC Industrial Supply Co., Melville, NY, USA) was used as the coolant (diluted with water at 1 to 20 ratio).

The workpiece material was titanium alloy (Ti-6Al-4V) provided by Boeing Company. The properties are shown in Table 2. The size of workpieces was $115 \times 85 \times 7.2$ mm. Diamond core drills were provided by N.B.R. Diamond Tool Corp. (LaGrangeville, NY, USA). The outer and inner diameters of the core drills were 9.6 mm and 7.8 mm, respectively. The mesh size of the diamond abrasives was 80/100. Three sets of experiments were conducted with three identical tools. Figure 5 illustrates the cutting tool. Three machining variables (spindle speed, feedrate, and ultrasonic power) were

TABLE 1 Experimental Conditions

Order of tests			Spindle speed ($rev \cdot s^{-1}$)	Feed rate ($mm \cdot s^{-1}$)	Ultrasonic vibration power (%)
Tool 1	Tool 2	Tool 3			
1	1	1	66.7	0.06	40
2	2	2	33.4	0.06	40
3	3	9	100	0.06	40
4	4	10	50	0.06	40
5	5	11	66.7	0.06	40
6	6	12	66.7	0.25	40
7	7	3	66.7	0.14	40
8		4	66.7	0.19	40
9		5	66.7	0.06	60
10		6	66.7	0.06	40
11		7	66.7	0.06	30
12		8	66.7	0.06	50

studied at four different levels. One variable was varied at a time while keeping the other two variables constant.

Measurement Procedure

During rotary ultrasonic machining, the cutting force along the feed direction was measured by a KISTLER 9257 dynamometer (Kistler Instrument Corp, Amherst, NY, USA). The dynamometer was mounted atop the machine table and beneath the workpiece, as shown in Figure 4. The electrical signals from the dynamometer were transformed into numerical signals by an A/D converter. Then the numerical signals to measure the cutting force were displayed and saved on the computer with the help of LabVIEW (Version 5.1, National Instruments, Austin, TX, USA). The sampling frequency to obtain the cutting force signals was 100 Hz. A typical curve of cutting force versus time is shown in Figure 6. The cutting force reported in this paper is the maximum cutting force on the cutting force curve, as illustrated in Figure 6. The maximum cutting force, not the average cutting force, was selected as one of the variables investigated in almost all the

TABLE 2 Properties of Titanium Alloy (Ti-6Al-4V)

Property	Unit	Value
Tensile strength	GPa	950
Thermal conductivity	$W \cdot m^{-1} \cdot K^{-1}$	21
Melting point	K	1941 ± 285
Density	$Kg \cdot m^{-3}$	4510
Heat of fusion	$kJ \cdot kg^{-1}$	440
Coefficient of thermal expansion	K^{-1}	8.64×10^{-6}

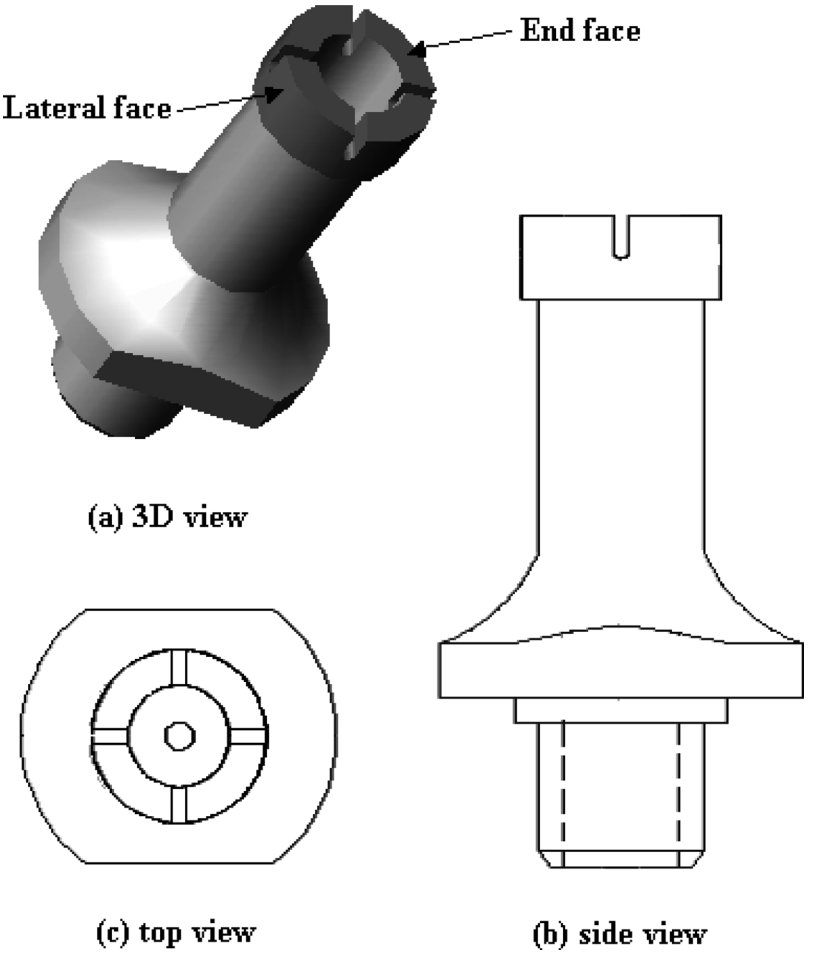

FIGURE 5 Illustration of the cutting tool for rotary ultrasonic machining.

previous studies (33–37). It is of the major concern because it determines the maximum stress in the workpiece, the maximum deflection or deformation of the machine, and the damage to the cutting tool.

The material removal rate (MRR) in the rotary ultrasonic machining was calculated using the following equation:

$$MRR = \frac{\text{Volume of material removed}}{\text{time}} = \frac{\pi \cdot [(D_{out}/2)^2 - (D_{in}/2)^2] \cdot d}{T} \quad (1)$$

where, D_{out} is the diameter of machined hole, D_{in} the diameter of machined rod, d workpiece thickness, and T the time it takes to drill the hole. Figure 7 illustrates the machined hole and rod.

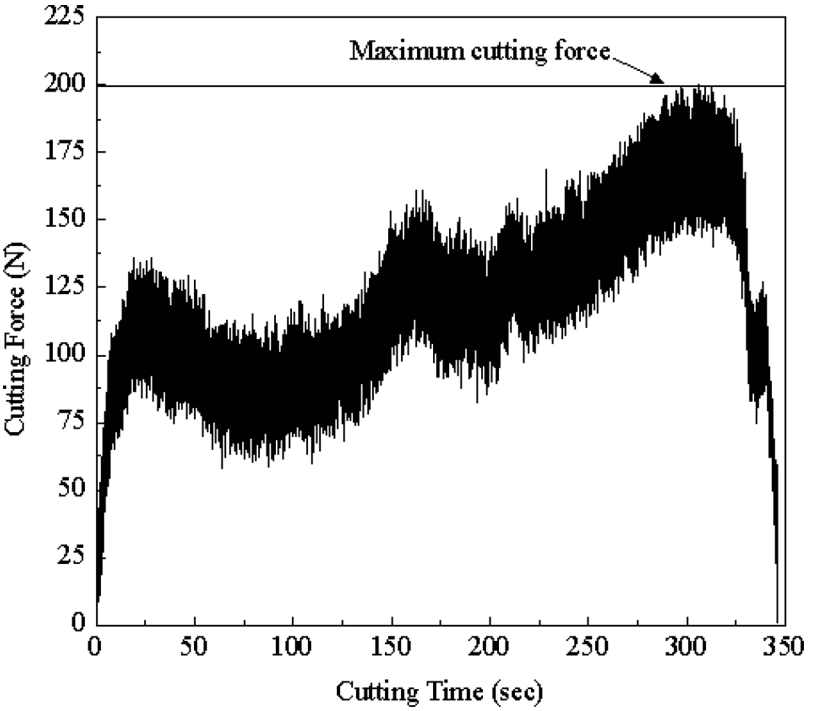

FIGURE 6 Measurement of maximum cutting force.

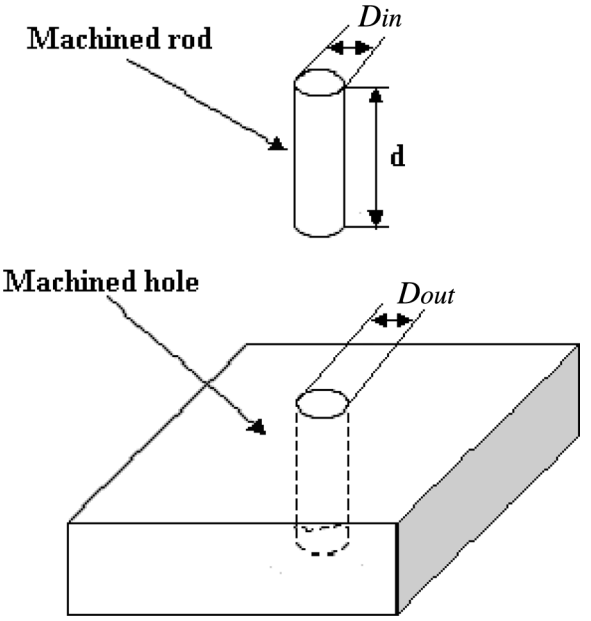

FIGURE 7 Illustration of the hole and rod machined by rotary ultrasonic machining.

FIGURE 8 Position of tool holding for observation of tool lateral face.

After each drilling test, the cutting tool was removed from the machine for observation under a digital microscope (Olympus DVM-1, Olympus America Inc., New York, USA). The magnification of the digital microscope was from 50 to 200. The topography was observed on both the end face and lateral face of the tool (see Figure 5). In order to ensure that the same area of the tool surface was observed every time, a special fixture was designed for holding the tool. The position shown in Figure 8 was for observation of the tool lateral face.

The surface roughness was measured on both the machined rod surface and the hole surface after each test with a surface profilometer (Mitutoyo Surftest-402, Mitutoyo Corporation, Kanagawa, Japan).

RESULTS AND DISCUSSION

In this section, the results of the experiments are presented. The software called MICROCAL ORIGIN (Version 6, Microcal Software, Inc., One Roundhouse Plaza, Northampton, MA, USA) was used to process the data. The cutting force, MRR, and surface roughness results are shown in Tables 3, 4, and 5, respectively.

Effects of Spindle Speed

On Cutting Force

The maximum cutting force vs. spindle speed curve is shown in Figure 9. The cutting force decreases significantly as the spindle speed increases.

TABLE 3 Results on Cutting Force (N)

Spindle speed ($rev \cdot s^{-1}$)	Feed rate ($mm \cdot s^{-1}$)	Ultrasonic vibration power (%)	Tool 1	Tool 2	Tool 3
66.7	0.06	40	118	111	123
33.4	0.06	40	547	534	565
100	0.06	40	98	102	97
50	0.06	40	298	264	244
66.7	0.06	40	118	119	134
66.7	0.25	40	680	750	695
66.7	0.14	40	390	385	402
66.7	0.19	40	448		468
66.7	0.06	60	145		138
66.7	0.06	40	118		106
66.7	0.06	30	161		172
66.7	0.06	50	109		101

TABLE 4 Results on MRR ($mm^3 \cdot s^{-1}$)

Spindle speed ($rev \cdot s^{-1}$)	Feed rate ($mm \cdot s^{-1}$)	Ultrasonic vibration power (%)	Tool 1	Tool 2	Tool 3
66.7	0.06	40	0.56	0.418	0.47
33.4	0.06	40	0.582	0.447	0.481
100	0.06	40	0.539	0.441	0.464
50	0.06	40	0.539	0.43	0.487
66.7	0.06	40	0.56	0.49	0.56
66.7	0.25	40	1.68	2.01	1.81
66.7	0.14	40	1.27	1.3	1.28
66.7	0.19	40	1.4		1.5
66.7	0.06	60	0.565		0.474
66.7	0.06	40	0.56		0.452
66.7	0.06	30	0.591		0.448
66.7	0.06	50	0.567		0.452

TABLE 5 Results on Surface Roughness (μm)

Spindle speed ($rev \cdot s^{-1}$)	Feed rate ($mm \cdot s^{-1}$)	Ultrasonic vibration power (%)	Tool 1		Tool 2		Tool 3	
			Hole	Rod	Hole	Rod	Hole	Rod
66.7	0.06	40	0.69	0.48	0.76	0.5	0.75	0.52
33.4	0.06	40	2.01	1.75	1.98	1.8	1.93	1.69
100	0.06	40	0.63	0.3	0.65	0.31	0.58	0.33
50	0.06	40	1.29	0.93	1.35	0.88	1.31	0.94
66.7	0.06	40	0.69	0.48	0.79	0.48	0.81	0.54
66.7	0.25	40	4.64	3.51	4.23	3.8	4.19	3.89
66.7	0.14	40	1.27	0.7	1.19	0.63	1.22	0.69
66.7	0.19	40	2.91	2.32			2.79	2.2
66.7	0.06	60	0.63	0.28			0.58	0.22
66.7	0.06	40	0.69	0.48			1.01	0.5
66.7	0.06	30	1.66	1.44			1.47	1.89
66.7	0.06	50	0.66	0.31			0.57	0.35

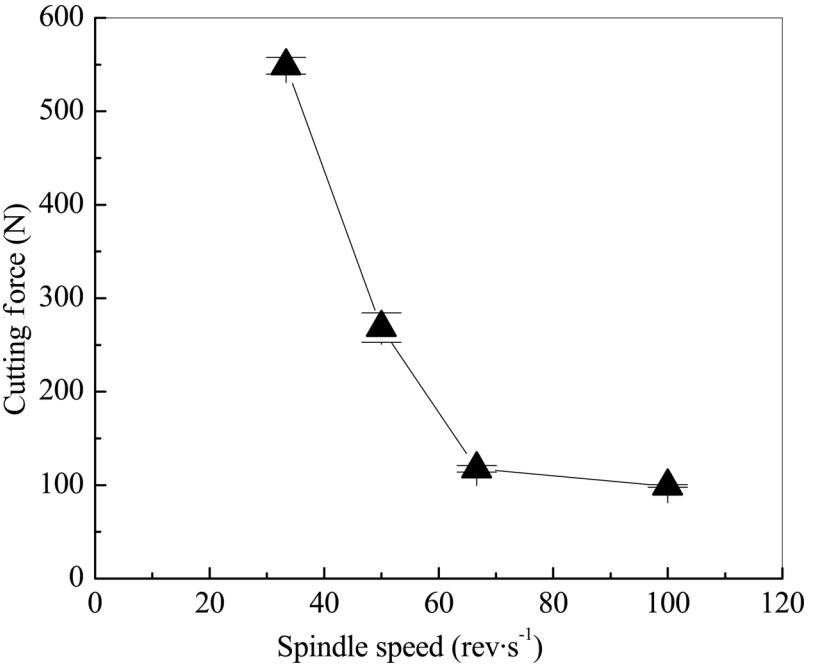

FIGURE 9 Effects of spindle speed on cutting force.

These results are consistent with those reported by Jiao et al. (33) for rotary ultrasonic machining of alumina. However, it is interesting to notice that these results are different from those reported by Li et al. (34). They reported that the spindle speed did not have significant effects on cutting force for rotary ultrasonic machining of ceramic matrix composite materials. Therefore, it can be said that the effects of spindle speed on cutting force vary for different workpiece materials.

It is also observed that the rate of decrease in the cutting force decreases when the spindle speed increases. In summary, the spindle speed has significant effects on cutting force; the lower the spindle speed, the higher the cutting force.

On Material Removal Rate (MRR)

The effects of spindle speed on MRR are shown in Figure 10. It can be seen that the spindle speed has no obvious effects on MRR. This is consistent with the results reported by Jiao et al. (33) for rotary ultrasonic machining of alumina. However, it is interesting to notice that this observation is different from those previously reported by Li et al. (34). They found that MRR increases as the spindle speed increases for rotary ultrasonic machining of ceramic matrix composite materials.

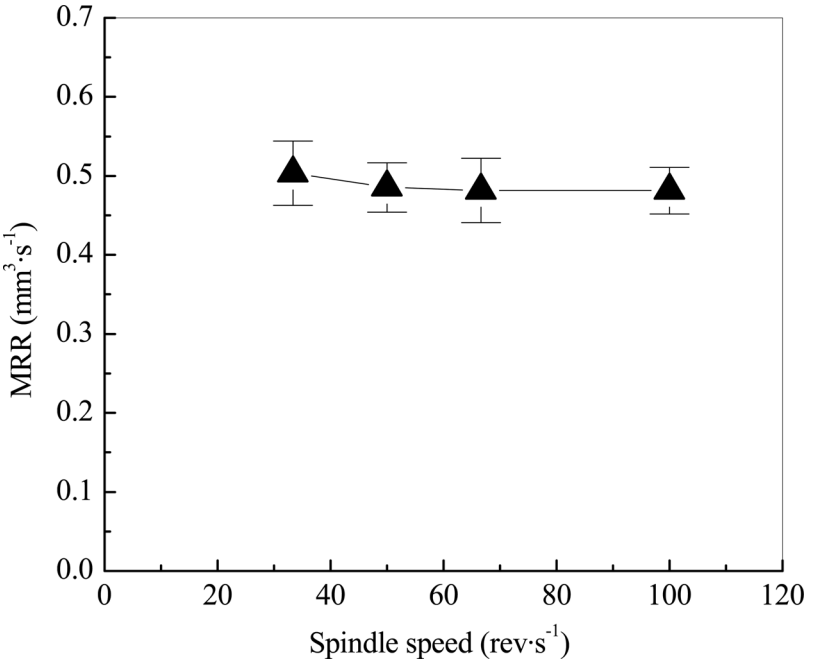

FIGURE 10 Effects of spindle speed on MRR.

On Surface Roughness Measured on the Machined Hole

The surface roughness curve for the machined hole is depicted in Figure 11. The surface roughness becomes significantly lower as the spindle speed increases. This observation is consistent with those reported by Jiao et al. (33) for rotary ultrasonic machining of alumina. It is also observed that the rate of decrease of surface roughness decreases with the increase in spindle speed. It can be concluded that spindle speed has significant effects on surface roughness on the machined hole.

On Surface Roughness Measured on the Machined Rod

The surface roughness curve for machined rod is depicted in Figure 12. The surface roughness becomes significantly lower as the spindle speed increases. This observation is consistent with those reported by Jiao et al. (33) for rotary ultrasonic machining of alumina. It is also observed that the rate of decrease of surface roughness decreases with the increase in spindle speed. Compared with the machined hole, the surface roughness observed on the rod is lower. It is concluded that spindle speed has significant effects on surface roughness on the machined rod.

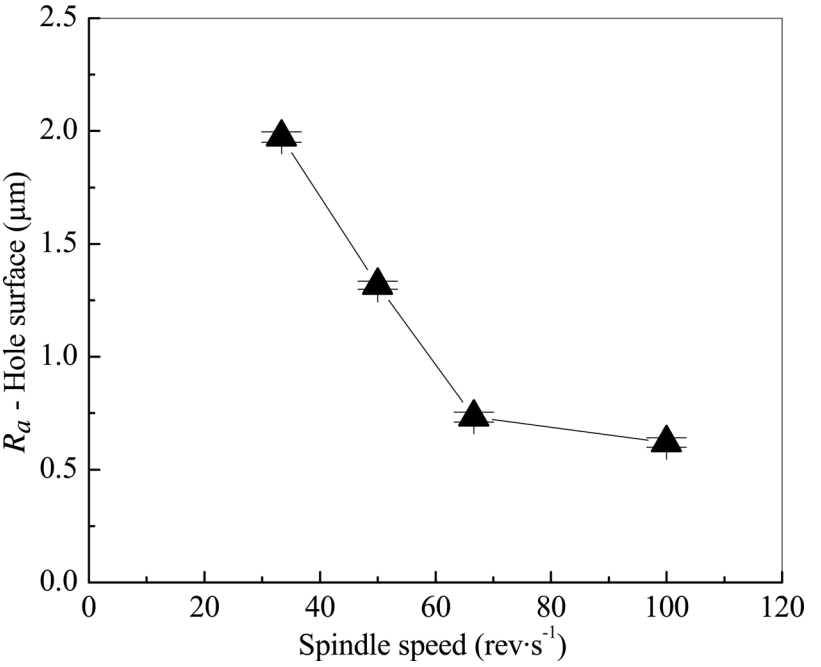

FIGURE 11 Effects of spindle speed on surface roughness measured on machined hole.

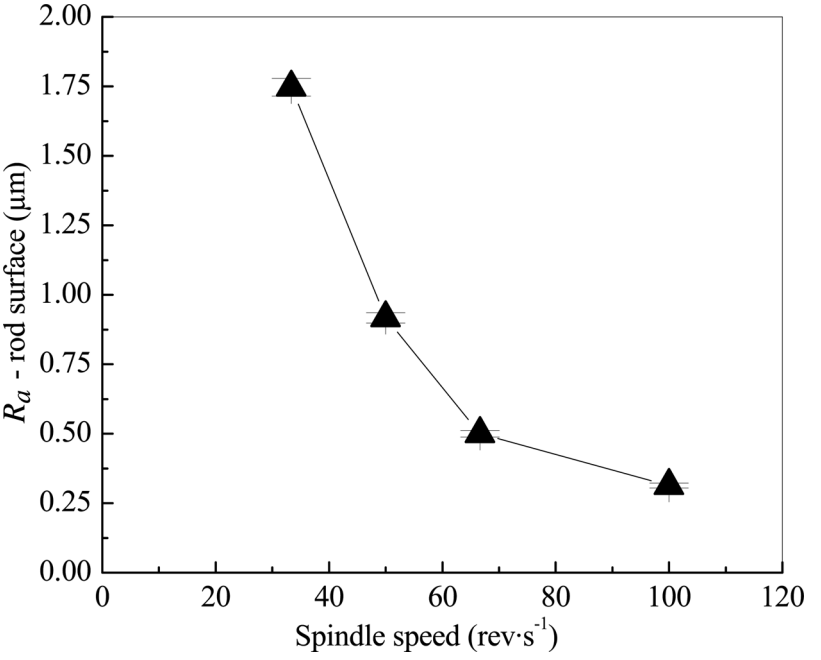

FIGURE 12 Effects of spindle speed on surface roughness measured on machined rod.

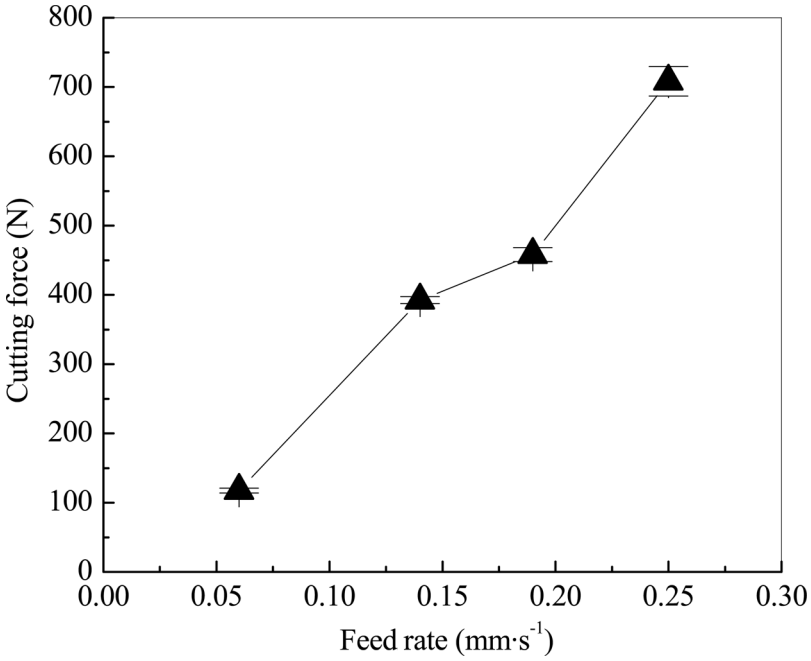

FIGURE 13 Effects of feed rate on cutting force.

Effects of Feed Rate

On Cutting Force

The feed rate has significant effects on cutting force, as shown in Figure 13. The cutting force increases significantly as the feed rate increases, which is consistent with the observation by Jiao et al. (33) and Li et al. (34) for rotary ultrasonic machining of alumina and ceramic matrix composite, respectively.

On Material Removal Rate (MRR)

As shown in Figure 14, when the feedrate increases, MRR increases. This is because that, as the feed rate increases, the tool travels faster in downward direction causing an increase in material removal rate. Jiao et al. (33) and Li et al. (34) reported a similar relationship between MRR and feed rate for rotary ultrasonic machining of alumina and ceramic matrix composite, respectively. Thus, even for different material properties, MRR always increases with feed rate.

On Surface Roughness Measured on the Machined Hole

The effects of feedrate on the machined hole surface roughness are depicted in Figure 15. The surface roughness measured on the hole increases significantly as the feedrate increases. This is consistent with the results from the study of Jiao et al. (33) for rotary ultrasonic machining of alumina.

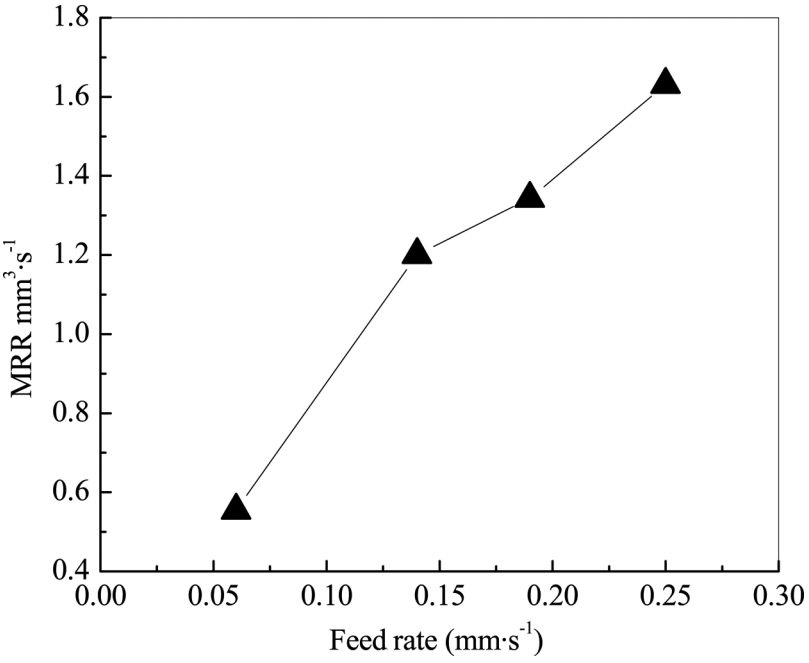

FIGURE 14 Effects of feed rate on MRR.

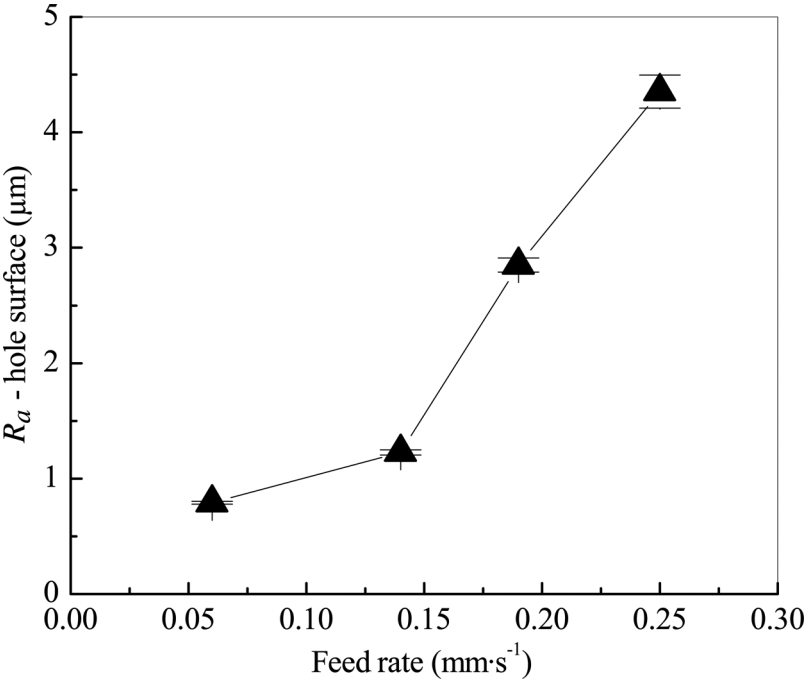

FIGURE 15 Effects of feed rate on surface roughness measured on machined hole.

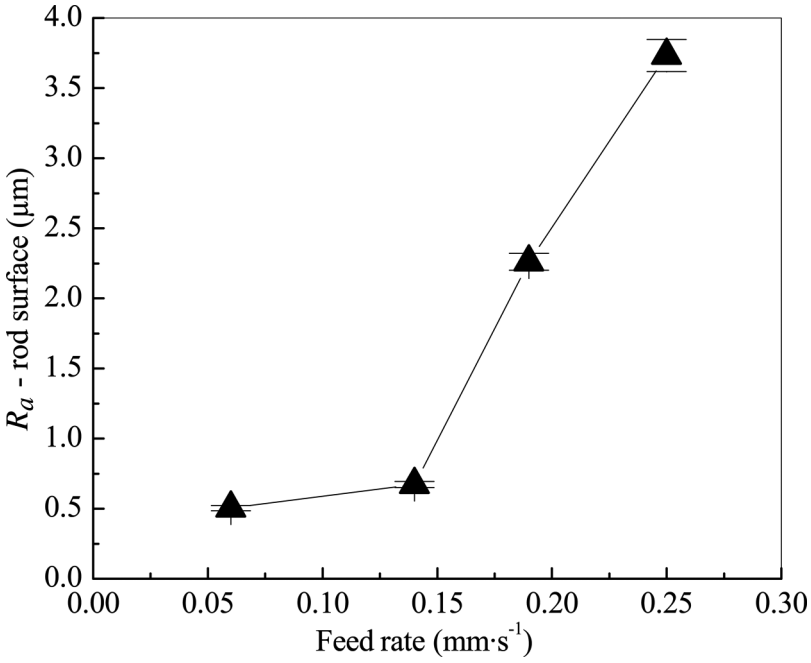

FIGURE 16 Effects of feed rate on surface roughness measured on machined rod.

On Surface Roughness Measured on the Machined Rod

The effects of feed rate on surface roughness on the machined rod are depicted in Figure 16. At lower feedrates, there is no significant increase in surface roughness. But at higher feed rates, the surface roughness increases significantly. The comparison of surface roughness values shows that roughness values for the machined rod are lower than those for the machined hole.

Effects of Ultrasonic Power

On Cutting Force

The ultrasonic power has significant effect on cutting force, as shown in Figure 17. Cutting force decreases initially as ultrasonic power level increases and then increases at the higher power level. This observation is different from those previously reported by Jiao et al. (33) and Li et al. (34). Jiao et al. found no significant effects of ultrasonic power on cutting force when rotary ultrasonic machining of alumina. Li et al. reported that cutting force increased as the ultrasonic power increased for rotary ultrasonic machining of ceramic matrix composites. Please note that both Jiao et al. and Li et al. used much smaller range of ultrasonic power (30–45% and 35–50% respectively) because they both used the two-level

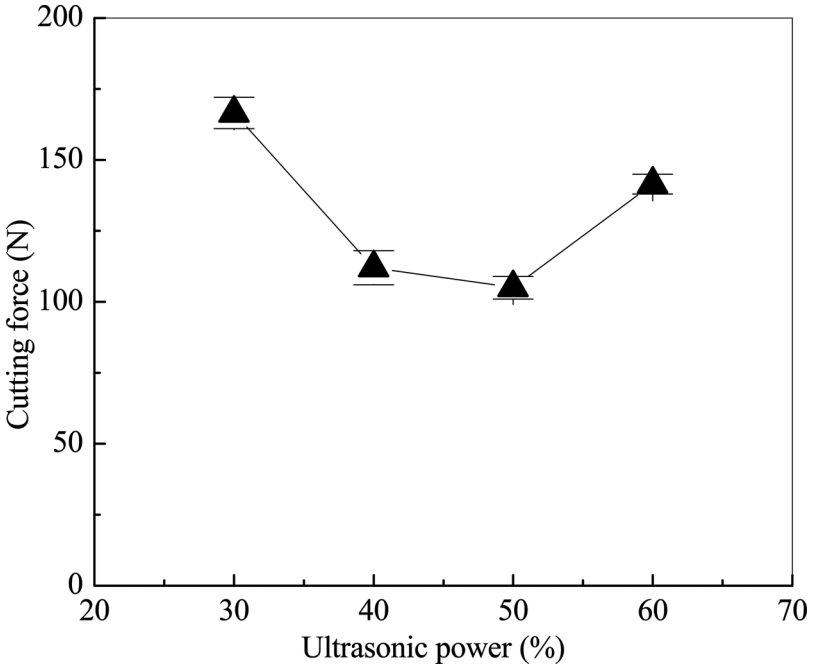

FIGURE 17 Effects of ultrasonic power on cutting force.

factorial design. One of the criteria to use the two-level factorial design is that the range of any factor has to be small enough to ensure that the response within the range is approximately linear.

On Material Removal Rate

The ultrasonic power has no significant effect on MRR, as shown in Figure 18. The MRR observed at various levels of ultrasonic power is almost constant. This is consistent with the results reported by Jiao et al. (33). However, it is interesting to notice that this observation is different from that reported by Li et al. (34). They reported that MRR increased as the ultrasonic power increased for rotary ultrasonic machining of ceramic matrix composites. The difference could be due to the fact that the variation associated with their composite drilling tests was relatively large. Note that, in their report, the significance level (α) for the effect of ultrasonic power on MRR was much larger than those for the effects of spindle speed and feedrate.

On Surface Roughness Measured on the Machined Hole

The effects of ultrasonic power on surface roughness measured on the machined hole are depicted in Figure 19. The surface roughness measured on the machined hole decreases significantly as the ultrasonic power increases. These results are consistent with those reported by Jiao et al. (33)

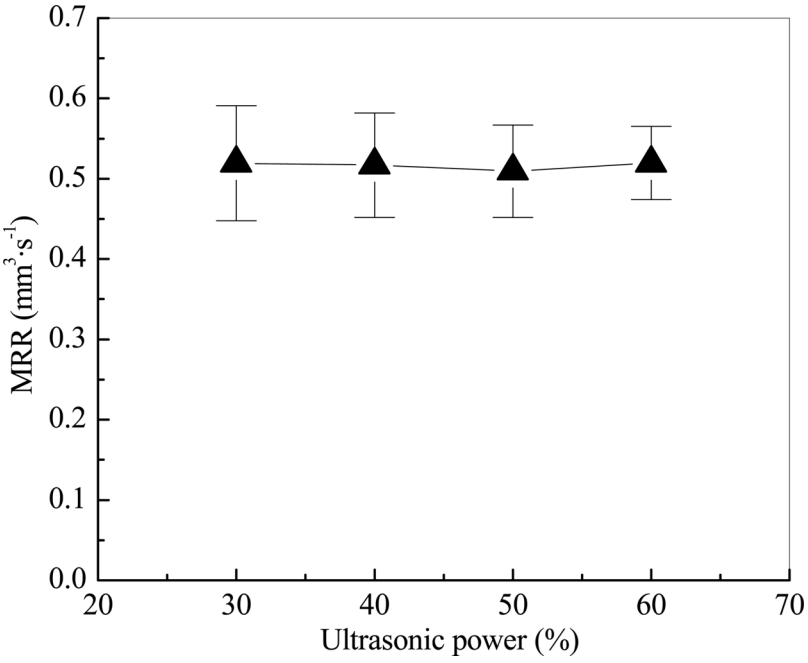

FIGURE 18 Effects of ultrasonic power on MRR.

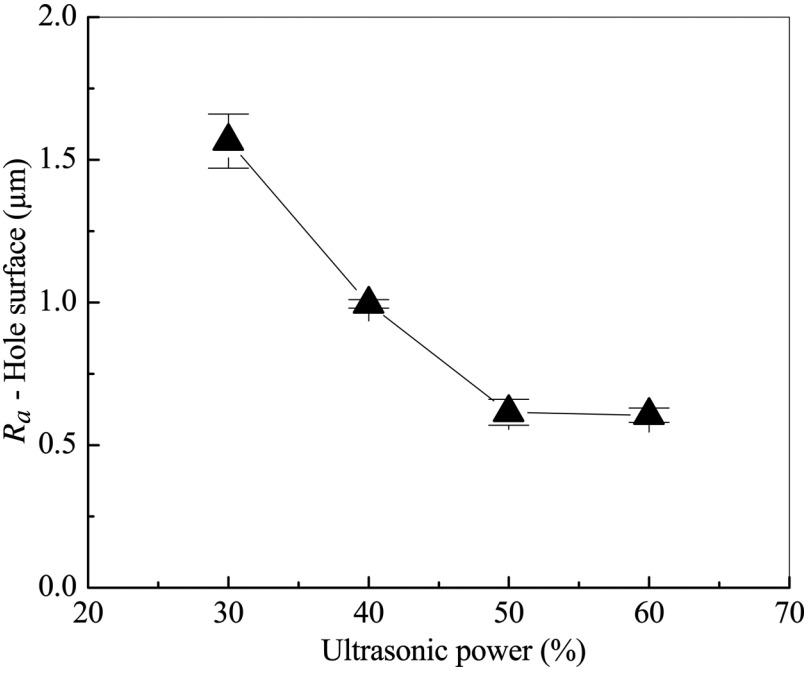

FIGURE 19 Effects of ultrasonic power on surface roughness measured on machined hole.

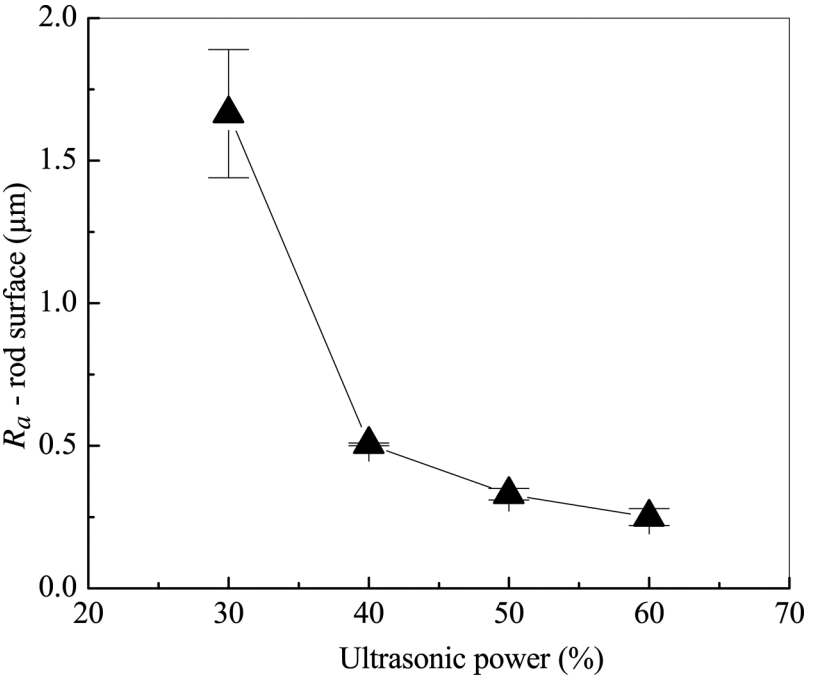

FIGURE 20 Effects of ultrasonic power on surface roughness measured on machined rod.

for rotary ultrasonic machining of alumina and by Li et al. (38) for rotary ultrasonic machining of technical glasses and advanced ceramics.

On Surface Roughness Measured on the Machined Rod

The effects of ultrasonic power on measured surface roughness measured on the machined rod are depicted in Figure 20. It is observed that as the ultrasonic power increases, the surface roughness measured on the rod surface decreases significantly.

CONCLUSIONS

In the present paper, the effects of three machining variables (spindle speed, feed rate, and ultrasonic power) on three output variables (cutting force, MRR, and surface roughness) while rotary ultrasonic machining of a titanium alloy are studied. The following conclusions can be drawn from the study:

1. The spindle speed has significant effects on cutting force and surface roughness, but its effects on material removal rate are not significant. Cutting force and surface roughness decrease as the spindle speed increases.

2. The feed rate has significant effects on cutting force, material removal rate, and surface roughness. Cutting force, material removal rate, surface roughness increases significantly as the feed rate increases.
3. The ultrasonic power has significant effects on cutting force and surface roughness, but its effects on material removal rate are not significant. Cutting force decreases initially and then increases as the ultrasonic power increases. Surface roughness decreases as the ultrasonic power increases.

ACKNOWLEDGMENTS

This work was supported in part by the Society of Manufacturing Engineers through a research initiation grant and by the Advanced Manufacturing Institute at Kansas State University. The authors gratefully extend their acknowledgements to Mrs. Tanni Sisco and Mr. Antonio Micale at Boeing Company for supplying the titanium alloy material; Mr. Bruno Renzi at N.B.R. Diamond Tool Corp. for supplying the diamond core drills.

REFERENCES

[1] Anonymous. (2000). Titanium Alloy Properties, available at: ⟨http://64.233.187.104/search?q=cache:cQz17heMf00J:www.roymech.co.uk/Useful_Tables/Matter/Titanium.html+&hl=en⟩.
[2] Froes, F., Allen, P., and Niinomi, M. (1998). Non-Aerospace Application of Titanium: An Overview. *Proceedings of Minerals, Metals and Materials Meeting, Minerals, Metals and Materials Society*, Warrendale, PA, pp. 3–18.
[3] Allen, K. (1997). Titanium Dioxide Pigment (and titanium metal), available at: ⟨http://www.chemlink.com.au/titanium.htm#Titanium%20metal⟩.
[4] Seddon, M. (2004). Titanium Demand Forecast to Recover with Increasing Aircraft Orders. Available at: ⟨http://www.roskill.com/news/newsCMS/newsItems/170604120648/viewNewsItem⟩.
[5] Huber, J. (1973). Ultrasonic Drilling. *International Journal for Numerical Methods in Engineering*, 5:28–42.
[6] Anonymous. (2004). *Report on Titanium, Common Minerals and Their Uses*. Mineral Information Institute, Denver, CO.
[7] Montgomery, J. and Wells, M. Titanium (2001) Armor Applications in Combat Vehicles. *Journal of Machining*, 53(4):29–32.
[8] Lerner, I. (2004). Titanium Market Recovering on Commercial Military Aircraft. *Chemical Market Reporter*, 266(18):17.
[9] Anonymous. (1989). New Automotive Materials. *Advanced Materials and Processes*, 135(1):6.
[10] Yamashita, Y., Takayama, I., Fujii, H., and Yamazaki, T. (2002). Applications and Features of Titanium for Automotive Industry. *Nippon Steel Technical Report*, 85:11–14.
[11] Farthing, T. (1979). Application of Titanium in the Chemical Industry. *Chemical Age of India*, 30(2):151–166.
[12] Orr, N. (1982). Industrial Application of Titanium in the Metallurgical Industries, and Chemical Light Metals. *Proceedings of Technical Sessions at the 111th American Institute of Mining, Metallurgical and Petroleum Engineers*, Annual Meeting, AIME, Warrendale, PA, pp. 1149–1156.
[13] Froes, F. (2002). Titanium Sport and Medical Application Focus. *Materials Technology*, 17(1):4–7.
[14] Abdullin, I., Bagautinov, A., and Ibragimov, G. (1988). Improving Surface Finish for Titanium Alloy Medical Instruments. *Biomedical Engineering*, 22(2):48–50.
[15] Yang, X. and Liu, R. (1999). Machining Titanium and its Alloys. *Machining Science and Technology*, 3(1):107–139.

[16] Anonymous. (1999). Weekly prices. *Platt's metal week*, 70(44):11.
[17] Nelson, O. (1991). Titanium Starves of Composites. *Advanced Materials and Processes*, 139(6):18–23.
[18] Li, E. and Johnson, W. (1996). Evaluation of Hybrid Titanium Composite Laminates for Room Temperature Fatigue. *Proceedings of American Society for Composites*, Lancaster, PA, pp. 505–514.
[19] Johnson, W. and Peker, A. (2003). Amorphous Alloy Surpasses Steel And Titanium. Available at: ⟨http://www.liquidmetal.com/news/dsp.news.11x304.asp⟩.
[20] Jenkins, M. (2003). Boeing puts the pedal to the metal, available at: ⟨http://www.boeing.com/news/frontiers/archive/2003/november/i_tt.html⟩.
[21] Kumar, K. (1996). Grinding Titanium. *Aerospace Engineering*, 11(9):17–19.
[22] Legge, P. (1964). Ultrasonic Drilling of Ceramics. *Industrial Diamond Review*, 24(278):20–24.
[23] Legge, P. (1966). Machining Without Abrasive Slurry. *Ultrasonics*, 4:157–162.
[24] Kubota, M., Tamura, Y., and Shimamura, N. Ultrasonic Machining with a Diamond Impregnated Tool. *Bulletin of Japan Society of Precision Engineering*, 11(3):127–132.
[25] Markov, A. and Ustinov, I. (1972). A Study of the Ultrasonic Diamond Drilling of Non-Metallic Materials. *Industrial Diamond Review*, 97–99.
[26] Markov, A. (1977). Ultrasonic Drilling and Milling of Hard Non-Metallic Materials with Diamond Tools. *Machine and Tooling*, 48(9):45–47.
[27] Petrukha, P. (1970). Ultrasonic Diamond Drilling of Deep Holes in Brittle Materials. *Russian Engineering Journal*, 50(10):70–74.
[28] Prabhakar, D. (1992). *Machining Advanced Ceramic Materials Using Rotary Ultrasonic Machining Process*. M.S. Thesis, University of Illinois at Urbana-Champaign.
[29] Prabhakar, D., Ferreira, P., and Haselkorn, M. (1992). An Experimental Investigation of Material Removal Rates in Rotary Ultrasonic Machining. *Transactions of the North American Manufacturing Research of SME*, 10:211–218.
[30] Wang, H. and Lin, L. (1993) Improvement of Rotary Ultrasonic Deep Hole Drilling of Glass Ceramics—Zerodur. *Seminar of the 7th International Precision Engineering*, Kobe, Japan, pp. 18–31.
[31] Pei, Z.J., Prabhakar, D., Ferreira, P., and Haselkorn, M. (1995). Mechanistic Approach to the Prediction of Material Removal Rates in Rotary Ultrasonic Machining. *Journal of Engineering for Industry*, 177:142–151.
[32] Pei, Z.J. and Ferreira, P. (1998). Modeling of Ductile-Mode Material Removal in Rotary Ultrasonic Machining. *International Journal of Machine Tools and Manufacture*, 38:1399–1418.
[33] Jiao, Y., Hu, P., Pei, Z.J., and Treadwell, C. (2005). Rotary Ultrasonic Machining of Ceramics: Design of Experiments. *International Journal of Manufacturing Technology and Management*, 7(2–4): 192–206.
[34] Li, Z., Jiao, Y., Deines, T., Pei, Z.J., and Treadwell, C. (2005). Rotary Ultrasonic Machining of Ceramic Matrix Composites: Feasibility Study and Designed Experiments. *International Journal of Machine Tools and Manufacture*, 45(12–13):1402–1411.
[35] Jiao, Y., Liu, W.J., Pei, Z.J., Xin, X.J., and Treadwell, C. (2005). Study on Edge Chipping in Rotary Ultrasonic Machining on Ceramics: An Integration of Designed Experiment and FEM Analysis. *Journal of Manufacturing Science and Engineering*, 127(4):752–758.
[36] Pei, Z.J. and Ferreira, P.M. (1999). An Experimental Investigation of Rotary Ultrasonic Face Milling. *International Journal of Machine Tools and Manufacture*, 39(8):1327–1344.
[37] Zeng, W.M., Li, Z.C., Pei, Z.J., and Treadwell, C. (2005) Experimental Observation of Tool Wear in Rotary Ultrasonic Machining of Advanced Ceramics. *International Journal of Machine Tools and Manufacture*, 45(12–13):1468–1473.
[38] Li, Z., Treadwell, C., and Pei, Z.J. (2004). *Drilling Small Holes in Hard-to-Machine Materials by Rotary Ultrasonic Machining*. SME Technical Paper TP04PUB137, Society of Manufacturing Engineers, Dearborn, MI.